JOURNAL OF GEOPHYSICAL RESEARCH, VOL. 105, NO. D11, PAGES 14,401–14,412, JUNE 16, 2000

Meridional distribution of hydroperoxides and formaldehyde in the marine boundary layer of the Atlantic (48°N-35°S) measured during the Albatross campaign

R. Weller and O. Schrems

Alfred Wegener Institut fur Polar- und Meeresforschung, Bremerhaven, Germany

A. Boddenberg and S. Gäb

Analytische Chemie, Bergische Universitat Gesamthochschule Wuppertal, Wuppertal, Germany

M. Gautrois

Institut für Atmosphärische Chemie, Forschungszentrum Jülich, Jülich, Germany

Abstract. Gas phase H_2O_2, organic peroxides, and formaldehyde (HCHO) have been measured in situ during October/November 1996 on board RV *Polarstern* in surface air over the Atlantic from 48°N-35°S with different analytical methods. The results indicate that recombination and self-reactions of peroxy radicals largely dominate over scavenging by NO. The peroxy radical chemistry was governed by the photooxidation of CH_4 and CO, as could be deduced from our failure to detect organic hydroperoxides other than CH_3OOH (methyl hydroperoxide (MHP)). Hydroperoxide and formaldehyde mixing ratios were highest within the tropics with peak values of around 2000 parts per trillion by volume (pptv) (H_2O_2), 1500 pptv (MHP), and 1000 pptv (HCHO). In the case of H_2O_2 and MHP we observed diurnal variations of the mixing ratios in the tropical North Atlantic and derived deposition rates of around $(1.8\pm0.6)\times10^{-5}$ s^{-1} for H_2O_2 and $(1.2\pm0.4)\times10^{-5}$ s^{-1} for MHP. The measured MHP/(H_2O_2+MHP) and MHP/HCHO ratios corresponded to 0.32±0.12 and 0.87±0.4, respectively. HCHO mixing ratios observed during the expedition were significantly higher than predicted by current photochemical theory based on the photooxidation of CH_4 and CO.

1. Introduction

Investigating photochemical processes in the marine troposphere, which covers around 70% of the Earth's surface is crucial to attain a detailed picture of tropospheric chemistry in a global sense, especially to assess the oxidation capacity of the atmosphere. In addition, this may help us in interpreting H_2O_2 and HCHO concentrations as recorded in ice and firn cores, which potentially provide restrictions concerning the oxidation capacity of the ancient troposphere [*Thompson et al.*, 1993a; *Staffelbach et al.*, 1991]. Large parts of the marine troposphere can be regarded as pristine and photochemical processes are mainly governed by the photooxidation of CO and CH_4 [*Thompson*, 1992]. It has been proven that photochemistry switches from a positive to a negative feed back on the O_3 concentration at NO levels lower than roughly 15 parts per trillion by volume (pptv) [*Crutzen and Zimmermann*, 1991] which is given in large parts of the troposphere, especially the marine boundary layer (MBL) [*Penkett et al.*, 1997; *Kley et al.*, 1996; *Singh et al.*, 1996; *Weller et al.*, 1996; *Platt et al.*, 1992]. As a consequence, recombination reactions of peroxy radicals (1)+(2) dominate over the competing reaction with NO (3):

Paper number 1999JD901145.
0148-0227/00/1999JD901145$09.00

$$HO_2 + HO_2 + M \rightarrow H_2O_2 + O_2 + M \quad (1)$$

$$HO_2 + ROO \rightarrow ROOH + O_2 \quad (2)$$

$$HO_2, ROO + NO \rightarrow OH, RO + NO_2 \quad (3)$$

This favors a pronounced formation of H_2O_2 and organic hydroperoxides (ROOH) in the remote MBL. Apart from the NO level, the absolute H_2O_2 and ROOH concentrations depend strongly on the UVB radiation intensity and the water vapor partial pressure because photooxidation of CH_4, CO, and nonmethan hydrocarbons (NMHC) as well as the formation of intermediate HO_2 and ROO radicals are initiated by OH radicals:

$$O_3 + h\nu(\lambda\leq320\text{nm}) \rightarrow O(^1D) + O_2 \quad (4)$$

$$O(^1D) + H_2O \rightarrow 2\,OH \quad (5)$$

Thus the H_2O_2 and ROOH formation is linked via peroxy-radicals with the so-called odd hydrogen family (OH, HO_2, H). According to *Kleinman* [1994] total hydroperoxide concentrations should exhibit for the low-NO_x case an almost linear dependence on the radical source strength. Major sinks are wet deposition and chemical degradation initiated by OH radical attack. In the MBL, dry and wet deposition are potentially the dominant H_2O_2 and ROOH losses [*Logan et al.*, 1981]. Field campaigns indicated that in the remote MBL the H_2O_2 budget is in fair agreement with this simple photochemistry [*Ayers et al.*, 1996; *Slemr and Tremmel*, 1994; *Junkermann and Stockwell*, 1999], although in more coastal

regions the influence of biomass-burning plumes as a source for NMHC and NO_x can be important [*Lee et al.*, 1997].

Hydroperoxide removal by deposition and OH attack dominates over photolytic odd hydrogen release, thus H_2O_2 and ROOH act primarily as peroxy-radical sinks. Concerning formaldehyde (HCHO), the photolysis channel yielding H-atoms and HCO-radicals is an important HCHO sink, comparable to the loss initiated by the reaction with OH. Thus HCHO must be regarded as an active radical source. The formation of HCHO at very low NO concentrations is not yet clarified [*Ayers et al.*, 1997]: The kinetics and the branching ratio into the HCHO-yielding reaction channels of the complex reactions CH_3OOH + OH [*Vaghjiani and Ravishankara*, 1989] and the CH_3OO self-reaction [*Kan et al.*, 1980] is somewhat uncertain, and a possible direct formation of HCHO by the reaction CH_3OO + HOO has been claimed [*Ayers et al.*, 1997]. As to the HCHO concentrations hitherto observed in the remote MBL, comparable investigations provided an inhomogeneous picture: some investigations indicated the observed HCHO mixing ratios to be less than predicted by simple photochemistry [*Lowe and Schmidt*, 1983; *Heikes et al.*, 1996], while others came to the opposite conclusion [*Arlander et al.*, 1995; *Ayers et al.*, 1997]. A recent study indicates that methane photooxidation is sufficient to describe the measured HCHO concentrations [*Junkermann and Stockwell*, 1999].

During the ALBATROSS campaign a wide range of trace gases has been measured above the Atlantic Ocean from high northern latitudes (68°N) to mid southern latitudes (42°S), yielding reliable trace gas distributions in this geographical area and providing valuable background data to assess certain photochemical processes in detail (H.P. Dorn, unpublished manuscript, 1999). Two groups, the Alfred Wegener Institute (AWI) and the Bergische Universität Gesamthochschule Wuppertal (BUGW), measured hydroperoxide concentrations by two different methods: high performance liquid chromatography (HPLC, BUGW) and a continuous dual-enzyme fluorimetric method (AWI). A comparison of the recorded data will be presented to assess the reliability of the measurements. Formaldehyde was determined by a continuous method (Hantzsch reaction, AWI). We will focus our interest on investigating the meridional distributions of hydroperoxides and HCHO mixing ratios, especially considering parameters characterizing the photochemical activity, transport and deposition processes. In addition, a speciation of organic peroxides will be given, and in a case study the hydroperoxide and HCHO distributions observed will be discussed in terms of a simple photochemical box model. Primary supporting data considered in this paper are the surface NO/NO_2, O_3, CO, and hydrocarbon distributions. Weather charts and 3-day back trajectories have also been made available by the German Weather Service (Deutscher Wetterdienst, DWD). The trajectory calculations are based on the global model of the DWD. In all cases the air masses reached the ship's position at 0000 UTC.

2. Methods and Instrumentation

2.1. Cruise Track and Experimental Setup

The measurements were performed on board the German research vessel RV *Polarstern*. The H_2O_2 and HCHO analyzers were installed inside air-conditioned laboratory containers set up on the forecastle (AWI). We have carefully chosen the location where we fixed our PTFE sampling lines to minimize the impact of seaspray. In order to keep the inlet orifices well clear of the ship, the HCHO inlet line was mounted on a 2 m boom fixed in front of the compass deck, where the cryogenic hydroperoxide sampling (BUGW) also took place. Two identical inlet lines for the H_2O_2 analyzer were mounted on the top of the air-chemistry container (15 m above sea level (asl)) on the ship's forecastle. In addition, we protected the inlets with a hood and inspected the lines daily. Trace-gas concentrations measured during relative wind directions outside a ±80° corridor with respect to the ship's heading and/or relative wind velocities <4 m/s could be affected by contamination originating from the exhaust plume of the ship. In such cases the NO/NO_x signals increased by 3-4 orders of magnitude and showed a strong variability within a concentration range of ≈1-20 ppbv, indicating the impact of a near local source (RV *Polarstern*). In parallel to the NO signal, the O_3 values decreased by about 30-50%, while the HCHO levels increased and both signals were highly fluctuating. The H_2O_2 mixing ratios, on the other hand, did not exhibit any striking response to such events.

The Atlantic traverse ANT XIV/1 of RV *Polarstern* started at Bremerhaven, Germany (54°N), on October 5 and ended at Punta Quilla, Argentina (50°S), on November 10, 1996. The itinerary of the cruise and the corresponding ground-level 3-day back trajectories are shown in Figure 1.

2.2. Hydroperoxide Measurements

2.2.1. Dual enzyme fluorimetric method. A fluorimetric method, described in detail by *Lazrus et al.* [1985] was applied for continuous quantification of hydroperoxides in ambient air. An air stream of 2000 cm^3 min^{-1} was drawn through the sampling line, a 4 mm ID PTFE hose. The instrument (Aerolaser H_2O_2 analyzer model AL1002, operated by the AWI) split the flow into two channels where H_2O_2 was stripped from the air by a buffer solution (pH=5.8). The stripping coil was a 50.2 cm long glass tube (ID 2 mm), and the flow rate of the stripping solution was regulated by a peristaltic pump at 0.42 cm^3 min^{-1}. In the first channel the fluorimetric reagent (para-hydroxyphenyl acetic acid (POPHA)) and peroxidase were added to determine the total amount of peroxides. POPHA forms a dimer when it reacts with H_2O_2/peroxidase and organic peroxides/peroxidase. The fluorescence of this dimer at 415 nm (excitation wavelength: 320 nm) provides a signal which is linearly dependent on the H_2O_2 concentration. Specific detection of H_2O_2 was achieved by selective destruction of H_2O_2 in the second channel with the enzyme catalase. During this expedition the HPLC- based hydroperoxide analyses revealed that no hydroperoxide other than methyl hydroperoxide (MHP, CH_3OOH) could be detected. Thus a continuous quantitative determination of MHP mixing ratios with the Lazrus method was feasible. However, a fraction of the organic peroxides is inherently destroyed by catalase, making a correction necessary. We evaluated the raw data in a way similar to that described by *Claiborn and Aneja* [1991]. The raw data from the peroxidase channel S_p and the signal of the catalase channel S_c was processed by the following expression:

$$[H_2O_2] = \frac{\alpha_0^k S_p - S_c}{\alpha_0^k - \alpha_0}, \quad [CH_3OOH] = \frac{S_c - \alpha_0 S_p}{\varepsilon(\alpha_0^k - \alpha_0)}$$

where α_0 is the residual H_2O_2 remaining in the catalase channel

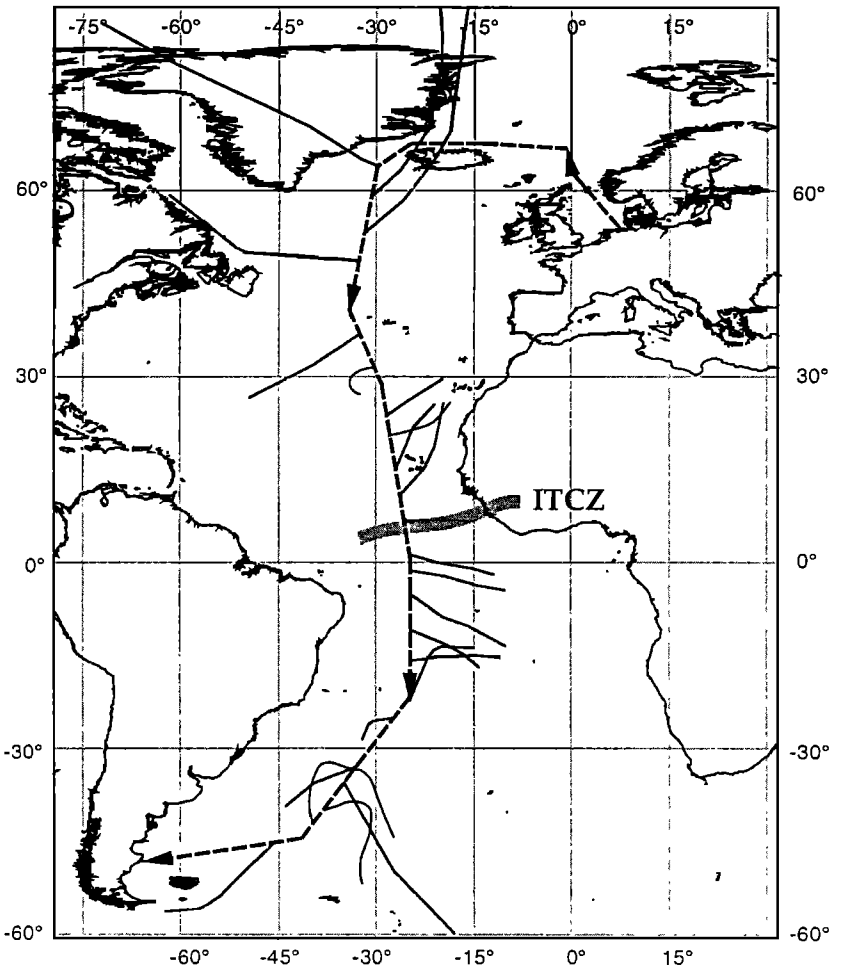

Figure 1. Itinerary of the *Polarstern* expedition ANT XIV/1. The location of the ITCZ corresponding to time when the ship passed the equator is indicated by the gray line. Also shown are surface 3-day back trajactories (arrival time: 0000 UTC) provided by the German Weather Service (Deutscher Wetterdienst, DWD).

and ε is the collection efficiency for MHP. Throughout the expedition the destruction efficiency of the catalase solution was determined daily and adjusted to between 85-95%, corresponding to α_0 = 0.15-0.05. The crucial factor is the ratio $K = k_i/k_0$ with k_i = pseudo first-order rate coefficient for catalase catalyzed decomposition of a mixture of hydroperoxides and k_0 for pure H_2O_2. Our laboratory investigations with standard solutions of pure MHP showed that at catalase efficiencies of 90% to 95% the MHP decay was around 5-7%, providing a value 0.017 for K. Another crucial factor is the collection efficiency ε of the stripping coil. Dimensions and stripping solution flow rate were exactly the same as described by *Lind and Kok* [1986]. With an airflow rate of 1000 cm^3 min^{-1} per coil, the gas and liquid phases are in equilibrium according to Henry's law [*Lind and Kok*, 1986]. Henry's law coefficients for H_2O_2 and MHP showed a strong temperature dependence [*Lind and Kok*, 1994]. The temperature inside the container was kept at 22°-24°C, except between 10°N and 0°S, where the temperature was raised to 26°C to prevent water condensation in the sampling lines (dew point in this region: 22°-25°C). Thus, for H_2O_2, the theoretical sampling efficiency was better than 99% throughout the cruise, whereas for MHP ε(299 K) = 0.67 and ε(295 K) = 0.76. To be conservative, we took a constant collection efficiency ε for MHP of 0.74±0.2.

The instrument was calibrated twice a day with standard solutions of 10^{-6} mol/L and 10^{-7} mol/L, freshly prepared from a stock solution of 10^{-2} mol/L H_2O_2. The concentration of the stock solution was determined by titration with $KMnO_4$ at the beginning and at the end of the cruise. The detection limit of the instrument was around 50 pptv. The efficiency of the PTFE inlet system on the forecastle, which was determined weekly, varied from 0.80 to 0.90 for H_2O_2 and around 0.95 for organic peroxides. This was determined by analysis of ambient air and air from a calibrated permeation source with and without the 4.5 m long PTFE line. To check the peroxide losses in the sampling line more frequently, the line in use was compared daily with the sealed, identical inlet system. Apart from the first leg north to around 20°N, where stormy weather was associated with heavy sea and large seasalt impact, the collection efficiency was constant at a ±5% level. When deviations greater than ±5% occured, the corresponding PTFE tube was cleaned with ultrapure water or changed. Taking into account the accuracy of the calibration, the instrument noise, the variability of the sampling line efficiency, and the catalase corrections, an instrumental accuracy of 15-20% at $[H_2O_2] \leq 500$ pptv, 12-15% at $[H_2O_2]$ = 500-2000 pptv, and around ±25% for MHP can be stated.

2.2.2. HPLC-method. The principal setup for the

quantification of H_2O_2 and organic hydroperoxides by means of HPLC is described in detail by *Hellpointner and Gäb* [1989]. Hydroperoxides were sampled by cryogenic enrichment at -80°C (sampling volume: 0.12 m^3 ambient air, sample flow: 50 cm^3/s) in a U-tube equipped with a glass fritt in the outlet arm (inlet 20 mm ID, outlet 10 mm ID, length 285 mm). Sampling at -80°C minimizes artifact hydroperoxide formation in the trap by condensed ozone [*Staffelbach et al.*, 1995]. The sample was cautiously thawed out at 20°C under running water and immediately injected via a 20-µL sample loop into the HPLC system. In both systems isocratic pumps (Merck Hitachi type 655A-11) were used for eluent delivery (0.5 mL/min of ultrapure H_2O/H_3PO_4 at pH=3.5). Before use, the eluent was degassed with high-purity helium (99.999%). The hydroperoxides were separated on a 5-µm LiChrospher ODS column (4 mm ID, 250 mm length, Merck). Detection of the hydroperoxides was achieved by two different methods: UV-absorption and fluorescence. To yield a fluorescent or UV-active product, the column effluent was mixed with specific reagent solutions and passed a stainless-steel reaction capillary (0.25 mm ID, 4 m length for fluorescence detection and 8 m length for UV detection). Fluorescence (λ_{ex}=190 nm, λ_{em}=415 nm) was measured by an HP 1056A fluorescence detector and UV-VIS absorbance at λ =253 nm by a Shimadzu SPD-6A UV-VIS detector. The fluorescence reagent was a solution of 40 mg horseradish peroxidase and 16 mg p-hydroxyphenyl acetic acid in a liter 0.01 *M* K_2HPO_4 buffer. A solution of 2000 mg N,N-dimethyl-1,4-phenylene-diammonium dichloride and 1400 mg $(NH_4)_2Fe(SO_4)_2$ in degassed 8.2×10^{-3} *M* H_2SO_4 solution was used as UV reagent. In both systems the detection limits were determined to be 20 pptv for H_2O_2, 40 pptv for MHP, and between 60 pptv and 90 pptv for other organic hydroperoxides. For calibration, pure MHP was synthesized by the method of *Williams and Mosher* [1954]. The purity of the H_2O_2 (30%) and MHP was determined by a photometric method [*Cramer et al.*, 1991]. Aqueous standards were prepared daily by dilution of 30% H_2O_2 and the MHP stock solution.

2.3. Formaldehyde Measurements

The quantification of HCHO was based on the so-called Hantzsch reaction, a liquid phase reaction of HCHO with 2,4-pentanedione and NH_3, yielding 3,5-diacetyl-1,4-dihydrolutidine. Formaldehyde is quantified fluorimetrically by exciting the end product of the reaction at 253 nm and 400 nm (Hg-lamp) and detecting the fluorescence at 510 nm. The analytical technique is described in detail by *Dasgupta et al.* [1988]. In this device (Aerolaser HCHO analyzer model AL4001, operated by the AWI), gaseous HCHO was stripped from a 1500 ccm min^{-1} airflow by acid solutions (0.05 N H_2SO_4). The stripping coil was thermostatted at 16°C, whereas the chemical reactor and the fluorescence cells were kept at a constant temperature of 60°C. The instrument was calibrated every 3 hours by an internal permeation source (para-formaldehyde, KIN-TEK™). The permeation source itself was calibrated every week by standard solutions of 10^{-6} mol/L HCHO, freshly prepared from a stock solution of 10^{-2} mol/L HCHO. The concentration of the stock solution has been determined by iodometric titration at the begining and at the end of the cruise. A detection limit of approximately 30 pptv is generally achievable, but on board the signals turned out to be much noisier than usual. This was largely due to a considerable blank signal caused by HCHO contamination in the ultrapure water used. Thus signals higher than 3σ of the standard deviation of the noise level corresponded to a poorer detection limit of 50-80 pptv. For HCHO it turned out that the sampling efficiency of the PTFE inlet system was not so critical as for the H_2O_2 measurements, and throughout the cruise a value of 0.95-0.98 was determined. We calculated the accuracy of the instrument to be 15-20% at [HCHO] ≤ 200 pptv and 10-15% at [HCHO] = 200-1000 pptv.

2.4. Supporting Trace Gas Measurements: NO/NO_2, CO, and Hydrocarbons

NO was measured continuously by the AWI with a chemiluminescence detector. The air samples have been taken via a PTFE hose. A 5 µm PTFE filter was installed in front of the analyser inlet. The NO instrument (ECO Physics, CLD 780 TR) detected the fluorescence intensity in a flow reactor in which the ambient NO was converted by ozone to excited NO_2*. Further details concerning calibration, calculation of the accuracy, and the detection limit of the apparatus are given by *Weller and Schrems* [1996]. The specific conversion of NO_2 to NO by photolysis allowed the detection of NO_2 in a separate measurement cycle by the same method. The CLD 780TR switched every 200 s from the NO to the NO_2 measuring mode. In this mode, ambient air passed through a photolytic converter (ECO Physics, PLC 770), consisting of a quartz reactor with a volume of 200 cm^3. The converter was equipped with a high-pressure 300 W Xe-arc lamp and a special filter/mirror combination confining the photolytic spectral range to 320-420 nm. In this mode the sum signal NO plus converted NO_2 is determined. Finally, the NO_2 values were derived from the difference signal, taking into account the NO_2 conversion efficiency, which was determined every 2-3 days throughout the expedition to be in the range of 78%-72%. The calculated accuracy of the NO and NO_2 measurements was around ±2-3 pptv and ±4-5 pptv, respectively, and a detection limit (twice the standard deviation of the overall background signal [*Weller and Schrems*, 1996]) of 3-4 pptv NO and 5-6 pptv NO_2 can be derived. A detailed description of the experimental setup for the CO and hydrocarbon measurements is given by M.Gautrois et al. (unpublished manuscript, 1999).

3. Results

3.1. Hydroperoxides

Figures 2a-2c show the meridional distribution of surface H_2O_2 and MHP from 48°N to 35°S. For the continuous dual enzyme method, 20-min averages are presented. The HPLC method provided data points corresponding to an average over the sampling time of 40 min. In addition, hitherto unpublished results from the *Polarstern* cruise ANT X/8 (from Ushuaia, Argentina, 55°S, to Bremerhaven, 53°N) conducted by AWI during January/February 1993 with the same technique are presented in Figure 3. The characteristic features measured on ANT X/8 were an increasing H_2O_2 mixing ratio from higher latitudes towards the equator and a broad maximum of around 2500 pptv between the Tropic of Cancer and the Tropic of Capricorn, decreasing to 200-300 pptv at higher latitudes in both hemispheres. The recent transect revealed a more complicated structure: The highest hydroperoxide mixing ratios were detected within the tropics with maximum values around 25°N, at the equator, and around 20°S. A striking feature observed on both transects was a H_2O_2 minimum within the

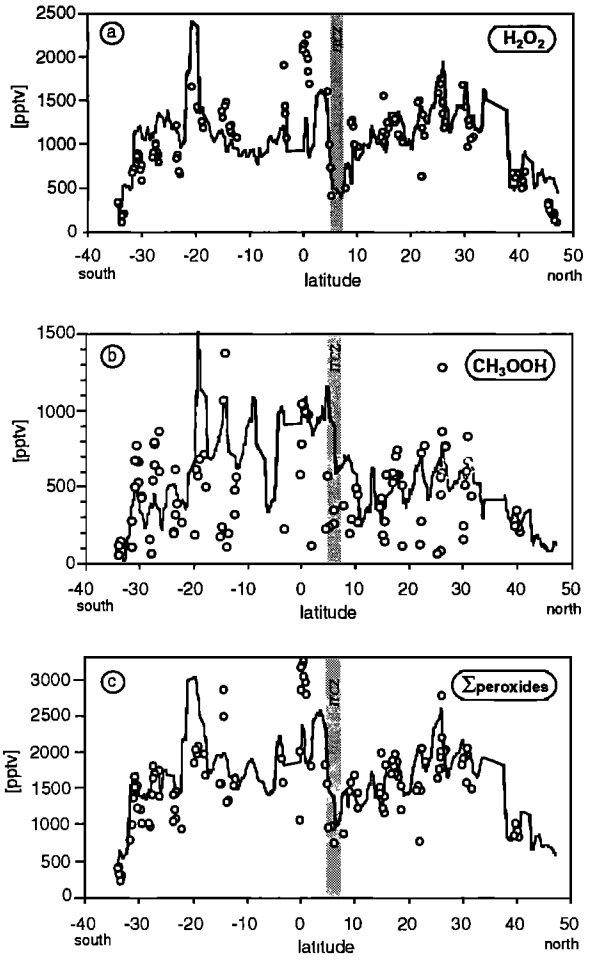

Figure 2. Meridional cross section of the (a) H_2O_2, (b) MHP, and (c) total amount of peroxides mixing ratios over the central Atlantic Ocean measured by the AWI (drawn line) and BUGW (circles). The interruptions were caused by technical problems and bad weather conditions.

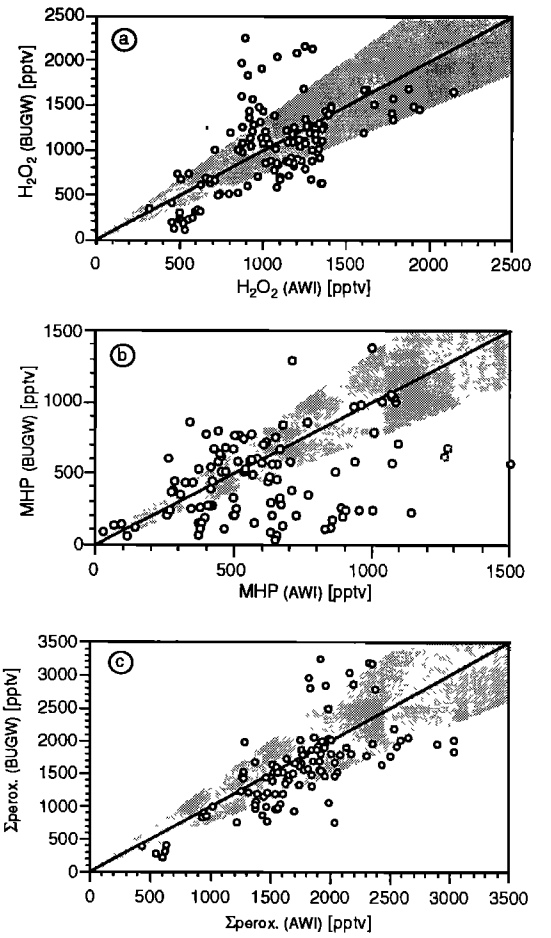

Figure 4. Comparison of the (a) H_2O_2, (b) MHP, and (c) total amount of peroxides mixing ratios measured by the two groups during the campaign. The shaded areas indicate corresponding ±25% error margins referring to the straight lines which represent perfect coincidence.

Intertropical Convergence Zone (ITCZ). The most crucial result derived from the HPLC-measurements was that organic hydroperoxides other than MHP were found to be below the detection limit of 60-90 pptv throughout the expedition. As to the H_2O_2 and MHP mixing ratios measured by the two groups, the shape of the meridional profile and the absolute values are in fair agreement: Concerning the observed total hydroperoxide, H_2O_2, and MHP mixing ratios, values of 70%, 65%, and 50%, respectively, were within a ±25% margin (Figures 4a-4c). The most striking difference between the dual enzyme and the HPLC method lies in the MHP data. Here the HPLC method sometimes showed a pronounced sample-to-sample variability.

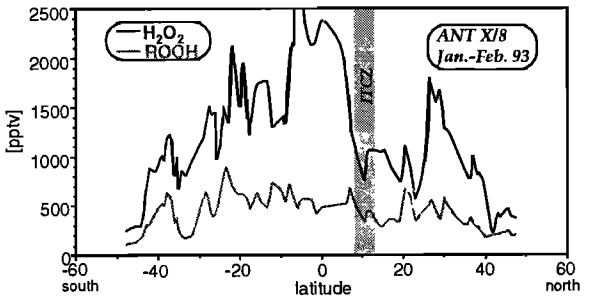

Figure 3. Latitude-dependent gaseous H_2O_2 and ROOH mixing ratios in the marine troposphere of the Atlantic Ocean, measured during *Polarstern* expedition ANT X/8 in January/February 1993.

3.2. HCHO Mixing Ratios

The meridional distribution of surface HCHO is presented in Figure 5. The individual data points correspond to 20 min averages. Like the meridional distribution of hydroperoxides, a broad maximum of around 1000-1200 pptv could be detected within the tropical Atlantic. Like the hydroperoxides, the meridional profile of the HCHO mixing ratios showed a minimum around the ITCZ.

3.3. NO and NO_2 Mixing Ratios

Because the hydroperoxide and HCHO photochemistry is highly dependent on the NO_x levels, we report the results of these measurements only in brief. The recorded NO and NO_2 mixing ratios (Figure 6) have been selected by a screening procedure where all data measured during relative wind

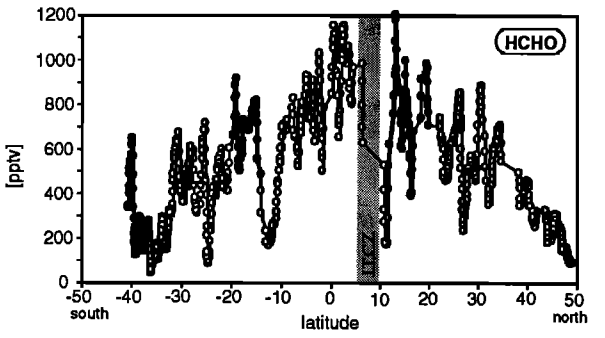

Figure 5. Meridional cross section of the observed HCHO mixing ratios over the central Atlantic Ocean. The interruptions were caused by technical problems and bad weather conditions. The data points marked as dots are influenced by the exhaust plume of RV *Polarstern*.

directions outside the ±80° corridor with respect to the ship's heading and/or relative wind velocities <4 m/s were discarded. With this screening procedure we could be sure of probing ambient NO_x which was not affected by contamination originating from the ship. However, this procedure is inherently subject to a small probability of throwing out good data. In the end, 80% of the recorded data remained for further evaluation. The NO and NO_2 levels observed in the remote MBL were extremely low during the whole cruise, with mean daytime NO mixing ratios of 3.1 pptv (range: 0-22 pptv, σ = 4.4 pptv) and mean NO_2 mixing ratios of 7.5 pptv (range: 0-27 pptv, σ = 13 pptv). A distinct maximum found between 10°N and 2°S may be caused by advection of air masses influenced by biomass burning from northern Africa. Within this zone the mean NO_2 and daylight NO mixing ratios increased to 15 pptv (σ = 11 pptv) and to 6.8 pptv (σ = 3.7 pptv), respectively. Comparable low NO mixing ratios in the MBL have been observed by *McFarland et al.* [1979] and by *Torres and Thompson* [1993] in the equatorial Pacific and by *Heikes et al.* [1996] over the South Atlantic. The NO and NO_2 mixing ratios found by *Rohrer and Brünning* [1992] during a meridional transect across the Atlantic were significantly higher, i.e. around 10 pptv NO and 25 pptv NO_2. It should be noted that *Rohrer and Brünning* [1992] could also observe higher NO and NO_2 levels within the 10°N to 0°N zone.

4. Discussion

4.1. Hydroperoxides

4.1.1. Comparison of the data. The hydroperoxide data set measured during the *Albatross* campaign, taken as a whole, supports quite well the conclusions drawn by *Staffelbach et al.* [1996] from a thorough comparison of different hydroperoxide measurement methods. The greater portion of the measured hydroperoxide mixing ratios are well within a ±25% margin which was roughly the combined experimental error of the different methods. However, there were extended periods in which differences of more than a factor of 2 could be observed. Particularly during periods of striking variations of the MHP mixing ratios as determined by HPLC, the differences for both H_2O_2 and MHP from the dual enzyme methods were far beyond the quoted experimental error. The same peculiarity was observed by *Staffelbach et al.* [1996]. Since the H_2O_2 mixing ratios measured by HPLC did not exhibit such a behavior, a photochemical explanation of this peculiarity seems unlikely. We tentatively hypothesize that these variations were caused by temperature instabilities of the cryogenic sampling technique. The dual enzyme technique, on the other hand, is potentially prone to serious errors if large amounts of different organic peroxides are present [*Kleindienst et al.*, 1988]. However, in our case, where only MHP could be detected and the dual enzyme procedure for discriminating H_2O_2 and MHP has proven to be a suitable method [*Staffelbach et al.*, 1996], one has to be aware that the MHP stripping efficiency is somewhat uncertain [*Heikes*, 1992]. Moreover, one has to consider the different sampling positions: the AWI inlet in particular was much more prone to the influence of sea spray during bad weather conditions. In fact, between 38°N and 34°N the AWI instrument had to be switched off because of stormy weather.

4.1.2. Meridional hydroperoxide distributions. The shapes of the profiles and the peak values of our observations are consistent with comparable measurements of gaseous hydroperoxides above the Atlantic [*Weller and Schrems*, 1993; *Slemr and Tremmel*, 1994; *Junkermann and Stockwell*, 1999]. Observations made by an independent technique, namely, tunable diode laser absorption spectroscopy, also showed maximum values around 1800 pptv at low latitudes [*Burrows et al.*, 1991]. However, *Jacob and Klockow* [1990] found significantly higher peak values on the order of 3500 pptv. Gaseous H_2O_2 mixing ratios of 630±280 pptv measured in the eastern subtropical North Atlantic by *Martin et al.* [1997] are comparable with the values observed during the *Albatross* campaign in this latitude range. In the tropical Pacific, considerably lower H_2O_2 and MHP mixing ratios of 600±180 pptv and 650±120 pptv, respectively, were found during the Soviet-American Gas and Aerosol Experiment (SAGA 3) campaign [*Thompson et al.*, 1993b].

From our measured NO mixing ratios it can be concluded that throughout the expedition the low NO_x criterion was given and that the hydroperoxide data were representative for the pristine MBL. Further evidence was given by the high $[H_2O_2]/[O_3]$ ratio, which was found to be 0.05±0.02. In rural regions influenced by advection of polluted air masses the $[H_2O_2]/[O_3]$ ratio is well below 0.02, typically around 0.005 [*Gilge et al.*, 1994]. Under pristine conditions, ambient H_2O_2 concentrations are dependent on the O_3 photolysis frequency, the H_2O partial pressure, and the H_2O_2 deposition rate. Decreasing solar UVB intensities and lower H_2O partial pressures over the cold water masses at higher latitudes seem

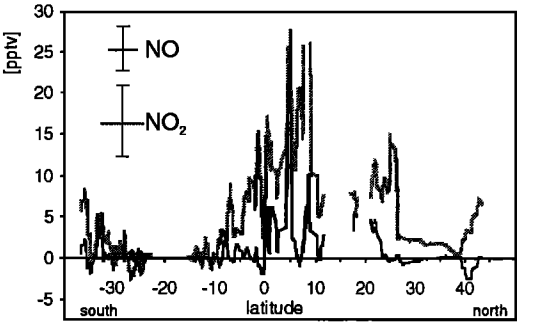

Figure 6. Meridional distribution of the NO (black line) and NO_2 (gray line) mixing ratios. Only the data measured during clean air conditions are presented.

Table 1. Ratio of MHP to the Total Amount of Hydroperoxides (MHP/(H_2O_2+MHP)) and the Standard Deviation (σ) of the Calculated Values

	MHP/(H_2O_2+MHP) ± σ (Range) Averages for the Whole Transect	MHP/(H_2O_2+MHP) ± σ Averages for the NH	MHP/(H_2O_2+MHP) ± σ Averages for the SH
AWI	0.32 ± 0.12 (0.1-0.6)	0.27 ± 0.06	0.36 ± 0.14
BUGW	0.30 ± 0.11 (0.11-0.55)	0.28 ± 0.10	0.32 ± 0.11

NH means the region north of the ITCZ, and SH is the region south of the ITCZ.

to be responsible for the more or less Gaussian shaped meridional H_2O_2 mixing ratio profile. A correlation between humidity or dew point, as suggested by *Calvert and Stockwell* [1983] is not given on the basis of our recent and former data [*Weller and Schrems,* 1993]. Interestingly, our results from comparable Atlantic traverses conducted on the *Polarstern* expeditions ANT X/1 [*Weller and Schrems,* 1993] and ANT X/8 showed a significant correlation between the H_2O_2 mixing ratio and the H_2O partial pressure, which can be expressed by the following empirical linear relations: H_2O_2[pptv] = 74×p(H_2O)[hPa]-317 (ANT X/1, coefficient of determination r^2=0.56), and H_2O_2[pptv] = 62×p(H_2O)[hPa]+17 (ANT X/8, r^2=0.62). In the tropical southern hemisphere the correlation was even more pronounced: H_2O_2 [pptv] = 103×p(H_2O)[hPa]-1021 (ANT X/1, r^2=0.69), and H_2O_2 [pptv] = 70×p(H_2O)[hPa]-85 (ANT X/8, r^2=0.8) Unfortunately, no corresponding correlation of our recent data set could be found (r^2<0.3). Because of its high solubility in water, the concentration of gaseous H_2O_2 depends strongly on the meteorological situation. To assess the dependence of the locally measured H_2O_2 mixing ratios on the H_2O partial pressure, it is especially important to know the meteorological history of the advected air mass. As a consequence, any correlation between the locally observed H_2O_2 and H_2O mixing ratios could be obscured by preceding variabilities of wet and dry deposition efficiencies caused by the individual weather conditions. The influence of wet deposition on the H_2O_2 mixing ratios is well documented within the ITCZ where low values were typically measured

4.1.3. MHP/(H_2O_2+MHP) ratios. The ratio of the measured MHP to the total amount of hydroperoxides is comprised in Table 1. Assuming that the organic peroxide concentrations found in previous field campaigns across the Atlantic corresponded to MHP, our recent results are in good agreement with MHP/(H_2O_2+MHP) ratios in the range of 0.2-0.35 found on *Polarstern* cruises ANT X/1 [*Weller and Schrems,* 1993] and ANT X/8. The ratio of *Slemr and Tremmel* [1994] ranged between 0.17 and 0.98, resulting in an higher average value of 0.48±0.14. In the continental boundary layer, significantly lower organic peroxide/total peroxide ratios around 0.1 seem to be typical [*Heikes et al.*, 1987; *Barth et al.*, 1989], but higher NO_x and nonmethane hydrocarbons (NMHC) mixing ratios and different deposition rates of H_2O_2 and organic peroxides than those in the remote marine boundary layer can be advanced as possible reason for this finding. The MHP/H_2O_2 ratio is also dependent on the present CH_4/CO ratios because the photooxidation of CO yields only HO_2 radicals. During our campaign the CH_4/CO ratios in the southern hemisphere (SH) were on average 23% higher (range: 5-45%) than those in the northern hemisphere (NH) (M. Gautrois et al., unpublished manuscript, 1999). The observed difference of the MHP/(H_2O_2+MHP) ratio in the NH from that in the SH seems to be higher (Table 1), but considering the experimental uncertainty this finding is rather inconclusive.

4.1.4. Diurnal H_2O_2 and MHP variations and deposition rates. Between 30°N and 10°N, pronounced diurnal variations of the H_2O_2 and MHP mixing ratios were recorded (Figure 7). During the nighttime, H_2O_2 and MHP loss rates in the range of (1.5-3.7) $\times 10^{-2}$ pptv s^{-1} and (6.5-9.3) $\times 10^{-3}$ pptv s^{-1}, respectively, have been derived. From these values, corresponding pseudo first-order deposition rates could be calculated: $k_{dep}(H_2O_2)$ = (1.8±0.6) $\times 10^{-5}$ s^{-1} and k_{dep}(MHP) = (1.2±0.4) $\times 10^{-5}$ s^{-1}. The H_2O_2 deposition rate determined in this study is in very good agreement with the following results from comparable observations in the remote MBL: (0.5-1.6)x10^{-5} s^{-1} [*Martin et al.*, 1997], 0.7×10^{-5} s^{-1} [*Martin et al.*, 1997] (derived from SAGA 3 data), 1.0x10^{-5} s^{-1} [*Ayers et al.*, 1996], and 1.4×10^{-5} s^{-1} [*Heikes et al.*, 1996]. *Slemr and Tremmel* [1994] found a significantly higher H_2O_2 deposition rate of around 4×10^{-5} s^{-1}, which seems to be inconsistent with recent observations [*Junkermann and Stockwell*, 1999], while their estimated MHP deposition rate is nearly identical with the value presented here. The consistency of the values determined by various authors may suggest that for the MBL an H_2O_2 deposition rate of around 1.2×10^{-5} s^{-1} holds. However, we believe that this agreement is a bit fortuitous: Deposition rates are bulk parameters which depend on several factors, such as the wind velocity, which increases the air-sea exchange and provokes formation of sea spray

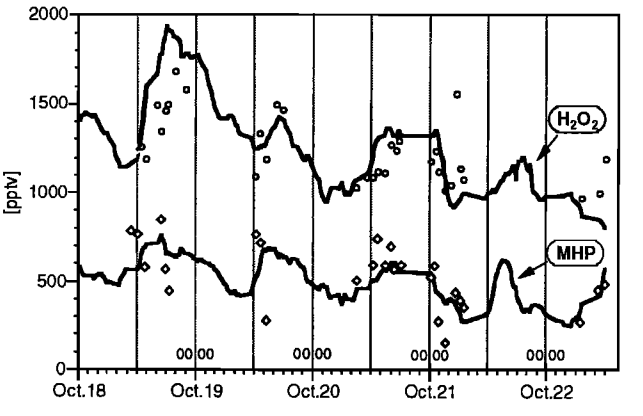

Figure 7. Diurnal variations of the (top) H_2O_2, and (bottom) MHP mixing ratios observed by the AWI and by the BUGW (open circles and diamonds, respectively) between 30°N and 10°N (October 18-22).

[*Liss and Merlivat*, 1986, *Deacon*, 1977], and the vertical mixing of the lower atmosphere, which is most pronounced during the night in the MBL. Furthermore, the height of the sample inlet above the sea surface can be very important, because of hydroperoxide scavenging by sea-spray produced by the ships movement. We emphasize that during this campaign diurnal variations were restricted to the tropical North Atlantic. Moreover, we could not detect any significant diurnal cycles during the cruises ANT X/1 and ANT X/8. Introducing a linear relation between the H_2O_2 deposition rate and wind velocity, *Slemr and Tremmel* [1994] successfully described their measured meridional H_2O_2 profile with simple steady state photochemistry. No such a relation could be confirmed by our recent observations. In fact, we did not find any statistically relevant correlation between the $k_{dep}(H_2O_2)$ and the wind velocity.

Although the difference between the deposition rates of MHP and H_2O_2 derived from our observations may not be significant considering the inherent uncertainty of the measurement, it is worthwhile to discuss this point separately. As far as dry deposition goes, the ocean is a perfect sink for MHP and H_2O_2, so that dry deposition rates are determined by the gas resistances [*Liss and Merlivat*, 1986; *Deacon*, 1977]. In this case the deposition velocities are dependent on the corresponding gas diffusivities, yielding a slightly lower dry deposition rate for MHP. As to wet deposition, measurements during ANT X/1 [*Weller and Schrems*, 1993] indicated that this removal process is again more efficient for H_2O_2. Therefore the overall deposition rate of H_2O_2 should be significantly higher than k_{dep}(MHP), as is consistent with our observation.

4.2. Formaldehyde

4.2.1. Meridional HCHO distribution. The shape of the meridional HCHO distribution and the daily mean mixing ratios are consistent with results derived from the differential optical absorption spectroscopy (DOAS) (T. Brauers, personal communication, 1999) and solar Fourier transform infrared (FTIR) spectroscopy experiment (J. Notholt et al., Latitudinal variations of trace gas concentrations measured by solar absorption spectroscopy during a ship cruise, submitted to *Journal of Geophysical Research*, 1999), but are obviously in contrast to the shipboard measurements performed by *Lowe and Schmidt* [1983] in October/November 1980 and by *Junkermann and Stockwell* [1999] on similar cruise tracks. The last two investigations report considerably lower HCHO mixing ratios, especially in the tropics. On the other hand, our results are in good agreement with airborne HCHO measurements during the Tropospheric Ozone (TROPOZ) II campaign [*Arlander et al.*, 1995]: In this study it could be shown that throughout the troposphere the HCHO levels were highest within the tropics. In these regions the HCHO mixing ratios in the MBL were found to be in the range of 600-1000 pptv, which is similar to our results. According to *Cohan et al.* [1999], HCHO mixing ratios in the tropical MBL in this magnitude should be a significant HO_x source for the upper troposphere by convective transport of HCHO. In another airborne study performed in the South Atlantic (Transport and Atmospheric Chemistry Near the Equator-Atlantic (TRACE-A) mission [*Heikes et al.*, 1996]), extremely low HCHO levels of 50-230 pptv were detected inside the MBL. However, only a few HCHO measurements could be conducted during this campaign. *Harris et al.* [1992] found HCHO mixing ratios of 470±200 pptv in the MBL over the North Atlantic in September/October, in agreement with our results in this region. Photochemical model calculations considering CH_4 as the only HCHO source predicted mixing ratios of around 350 pptv in the tropics and 100 pptv in polar regions [*Logan et al.*, 1981], which is significantly higher than the observations of *Lowe and Schmidt* [1983] and *Heikes et al.* [1996] but far lower than the results of *Harris et al.* [1992] and *Arlander et al.* [1995]. Model calculations including the photochemistry of nonmethane hydrocarbons (NMHC), yielded an HCHO distribution which is consistent with the TROPOZ II observations [*Arlander et al.*, 1995]. As determined in the *Albatross* campaign, however, the photochemistry of the measured NMHC concentrations did not indicate any significant influence on the locally measured HCHO mixing ratios: Between 45°N and 40°S the mixing ratios of the NMHCs C_2H_6 and C_3H_8 were below 800 pptv and 110 pptv, respectively (M. Gautrois et al., unpublished manuscript, 1999). It can be concluded that the total production rate of C_1-compounds through the photooxidation of C_2H_6 and C_3H_8 was less than 5% and thus negligible. This indicates that CH_4 photooxidation should be the dominant HCHO source to be considered here. On the other hand, photooxidation of more reactive unsaturated NMHCs like ethene (C_2H_4), propene (C_3H_6), and isoprene (C_5H_8), which were not determined during the *Albatross* campaign, yields HCHO directly. The influence of isoprene is most likely restricted to coastal areas with high biogenic activity [*Bonsang et al.*, 1992]. Mixing ratios of ethene and propene are highly variable in remote marine regions, ranging from about 20 pptv up to 100-300 pptv [*Singh and Zimmermann*, 1992]. Thus these compounds may potentially provide a substantial source for HCHO.

Because the photochemical lifetime of HCHO is of the order of hours, HCHO should be in local photochemical equilibrium [*Lowe and Schmidt*, 1983; *Arlander et al.*, 1995]. Long-range transport of HCHO can be neglected. Actinic radiation is also involved in the main HCHO sink: Photolysis and degradation by OH attack [*Lowe and Schmidt*, 1983]. Wet and dry deposition is believed to be of minor importance in the MBL [*Zafiriou et al.*, 1980], as is supported by the lack of any

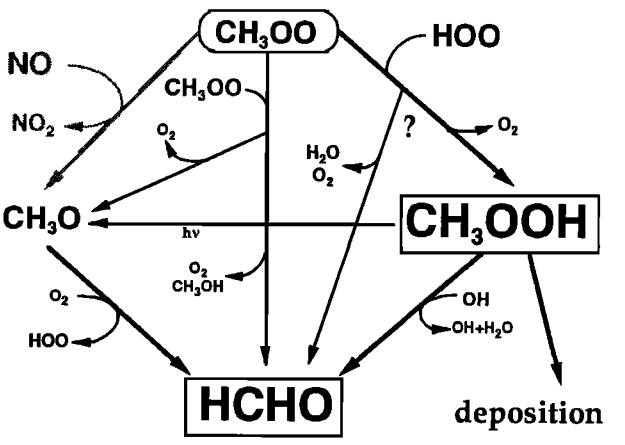

Figure 8. Possible reaction pathways yielding HCHO in the photooxidation of CH_4. In the pristine MBL the CH_3OO + NO pathway (gray) is of minor importance. Note that a direct HCHO formation by the reaction CH_3OO + HO2 increases the HCHO yield while HCHO formation via MHP is lowered by MHP deposition.

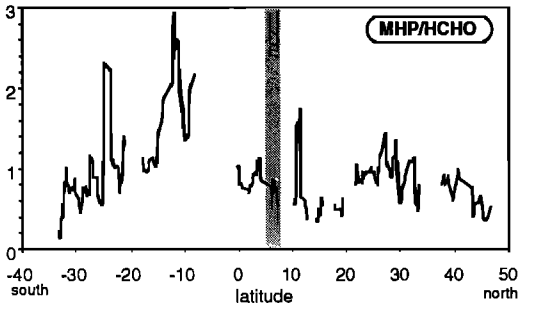

Figure 9. Meridional dependence of the MHP/HCHO ratio. Only the data measured during clean air conditions are presented.

diurnal HCHO variations throughout this expedition. This is in agreement with the results of *Junkermann and Stockwell* [1999]. However, *Lowe and Schmidt* [1983] could detect a diurnal HCHO cycle under stable weather conditions in the equatorial Atlantic and claimed dry deposition to be an important HCHO sink. Varying vertical stability of the MBL during night may have obscured a pronounced diurnal variation of HCHO levels. Thus it was impossible to estimate from our results, even on an order-of-magnitude scale, a reliable value for dry and wet deposition. From the measured daytime NO mixing ratios we further conclude that typically less than 25% of the HCHO present was produced via the CH_3OO + NO pathway (Figure 8): Taking into account an NO mixing ratio of 3 pptv, a daily mean HO_2 mixing ratio of 20 pptv (J. Burkert et al., unpublished manuscript, 1999), and the rate coefficients for the reactions CH_3OO + NO and CH_3OO + HO_2 (k_{298} = 4.6×10^{12} cm^3 mol^{-1} s^{-1} and k_{298} = 3.1×10^{12} cm^3 mol^{-1} s^{-1}, respectively [*Atkinson et al.*, 1992]), it turns out that only around 17% of the HCHO was formed via the NO pathway. This is supported by the high but strongly variable MHP/HCHO ratios of about 0.9 found throughout the expedition (Figure 9). However, from the MHP, HCHO, and NO_x measurements, no significant correlation between the MHP/HCHO ratio and the NO_x mixing ratios could be found.

4.2.2. Results from a photochemical box model. In the following approach, we aim to describe in terms of a case study the observed MHP and HCHO mixing ratios with the help of a photochemical box model (Table 2) based on the CH_4 and CO photooxidation in the MBL. We will restrict our simulations to the subtropical NH between 28°N and 24°N because within this region our hydroperoxide data are in good agreement (within ±15% for H_2O_2 and ±30% for MHP). Furthermore, trajectory analyses revealed that the advected air masses had not had any contact with land masses or even coastal regions for the last 3 days and quite stable fair weather conditions prevailed. The photolysis rates J used in the model represent daily means, neglecting diurnal variations. They are typical for this region and season and consistent with values actually derived from actinometric measurements. The mixing ratios employed for H_2O (0.025), O_3 (30 ppbv), CH_4 (1.8 ppmv), CO (85 ppbv), and NO_x (12 pptv) are representative of the data actually measured in this region. For H_2 a mixing ratio

Table 2a. Reaction Mechanism and Corresponding Rate Coefficients

Reaction									Rate Coefficient
O^1D	+	M		→	O^3P	+	M		1.70×10^{13}
O^1D	+	H_2O		→	2 OH				1.41×10^{14}
OH	+	O_3		→	HO_2	+	O_2		$1.10\times10^{12}\exp(-1000/T)$
HO_2	+	O_3		→	2 O_2	+	OH		$8.43\times10^{9}\exp(-600/T)$
HO_2	+	HO_2		→	H_2O_2	+	O_2		4.3×10^{12}
H_2O_2	+	OH		→	HO_2	+	H_2O		$1.75\times10^{12}\exp(-160/T)$
H_2	+	OH		→	H	+	H_2O		$4.63\times10^{12}\exp(-2100/T)$
HO_2	+	OH		→	O_2	+	H_2O		$2.90\times10^{12}\exp(+250/T)$
CO	+	OH		→	CO_2	+	H		1.44×10^{11} (a)
CH_4	+	OH		→	CH_3	+	H_2O		$1.6\times10^{12}\exp(-1800/T)$[a]
CH_3O_2	+	CH_3O_2		→	HCHO	+	$CH_3OH + O_2$		$7.4\times10^{10}\exp(+220/T)$[b]
CH_3O_2	+	CH_3O_2		→	$2CH_3O$	+	O_2		$5.6\times10^{10}\exp(+220/T)$[b]
CH_3O_2	+	HO_2		→	CH_3OOH	+	O_2		$2.30\times10^{11}\exp(+780/T)$
CH_3OOH	+	OH		→	HCHO + OH	+	H_2O		$6.0\times10^{11}\exp(+190/T)$
CH_3OOH	+	OH		→	CH_3O_2	+	H_2O		$1.14\times10^{12}\exp(+190/T)$
CH_3OH	+	OH		→	H_2O	+	prod.		$4.0\times10^{12}\exp(-600/T)$
CH_3O	+	O_2		→	HCHO	+	HO_2		$4.35\times10^{10}\exp(-1080/T)$
HCO	+	O_2		→	CO	+	HO_2		3.3×10^{12}
HCHO	+	OH		→	HCO	+	H_2O		$5.28\times10^{12}\exp(+25/T)$
HO_2	+	NO		→	OH	+	NO_2		$2.20\times10^{12}\exp(+240/T)$
CH_3O_2	+	NO		→	CH_3O	+	NO_2		$2.53\times10^{12}\exp(+180/T)$
O_3	+	NO		→	O_2	+	NO_2		$1.1\times10^{12}\exp(-1370/T)$
CH_3	+ O_2	+	M	→	CH_3O_2	+	M		$3.60\times10^{16}(T/298)^{-3.3}$
O	+ O_2	+	M	→	O_3	+	M		$2.20\times10^{14}(T/298)^{-0.28}$
H	+ O_2	+	M	→	HO_2	+	M		$2.20\times10^{16}(T/298)^{-1.60}$
H_2O_2				→	deposition				1.2×10^{-5}
CH_3OOH				→	deposition				0.8×10^{-5}
HCHO				→	deposition				1.0×10^{-5}

Rate coefficients are taken from *Atkinson et al.* [1992].

[a]Rate coefficient is taken from *DeMore et al.* [1994].

[b]Rate coefficient is taken from *Kan et al.* [1980] and *DeMore et al.* [1994].

Units: cm^3 mol^{-1} s^{-1} for bimolecular reactions and cm^6 mol^{-2} s^{-1} for termolecular processes. The effect of water vapor on the rate coefficient k(HO_2+HO_2) has been considered according to *Atkinson et al.* [1992].

Table 2b. Photolyses Reactions and Corresponding Photolysis Frequencies (Daily Mean)

Photolyses							Photolysis Frequency, s^{-1}
O_3	+	hv	→	O^1D	+	O_2	9.5×10^{-6}
NO_2	+	hv	→	O^3P	+	NO	3.2×10^{-3}
H_2O_2	+	hv	→	2OH			2.5×10^{-6}
HCHO	+	hv	→	CO	+	H_2	1.2×10^{-5}
HCHO	+	hv	→	HCO	+	H	0.8×10^{-5}
CH_3OOH	+	hv	→	CH_3O	+	OH	2.6×10^{-6}

of 585 ppbv was taken. The mixing ratios of these background gases were kept constant during the simulations. The model was run for 10 days, sufficient to reach photochemical equilibrium. The results clearly revealed that it is impossible to bring the measured high HCHO mixing ratios into accord with the calculations, even by varying the rate coefficients $k(CH_3OO+HOO)$ and $k(CH_3OO+CH_3OO)$ within the given margin of error [*Atkinson et al.*, 1992]. By setting the branching ratio of the reaction $CH_3OO + HO_2$ into the HCHO yielding channel to the proposed maximum value of 0.4 [*Jenkin et al.*, 1988] or enhancing the rate coefficients $k(MHP+OH\rightarrow HCHO+OH+H_2O)$ and $k(MHP+OH\rightarrow CH_3O_2+H_2O)$ to 2.6×10^{12} cm^3 mol^{-1} s^{-1} and 3.9×10^{12} cm^3 mol^{-1} s^{-1}, respectively [*Atkinson et al.*, 1989] we were able to get the model results to approach the values actually measured (Table 3). Note that the MHP/HCHO ratio in particular is now very close to the observed values, which could not be achieved by neglecting the reaction CH_3OO+HO_2. To check the significance of a NO depending HCHO yield, we also ran the model with an NO_x mixing ratio of 20 pptv instead of 12 pptv (Table 3). Clearly, within the given accuracy of the NO_x data, the observed MHP/HCHO can not be simulated with the standard mechanism. In addition, this simulation reveals the minor influence of NO_x within the observed concentration range on the MHP/HCHO ratio, independent of the mechanism used. Even considering the low accuracy of the NO and NO_2 mixing ratios which were close to the detection limit for large parts of the campaign, the observed meridional dependence of the MHP/HCHO ratio (Figure 9) was most probably not caused by corresponding variations of ambient NO_x mixing ratios. Concerning the MHP/(H_2O_2+MHP) ratio, the photochemical box model revealed that increasing the CH_4/CO ratios by 23% according to conditions typically observed in the SH (CH_4=1.75 ppmv, CO=65 ppbv) results in increasing MHP/(H_2O_2+MHP) ratios of 0.48, 0.36, and 0.37 for the standard reaction mechanism and the modifications, respectively (Table 3). Again, the model results are in better agreement with observations for the modified reaction schemes. The reason for the weak influence of the hemispheric CH_4/CO ratio difference on the MHP/(H_2O_2+MHP) ratio is the fact that OH attack of MHP is ≈3 times faster compared to H_2O_2 and the photochemical decay of MHP to CO_2 yields additional HOO radicals which mainly recombine to H_2O_2.

Ayers et al. [1997] also pointed out the relevance of the HCHO-yielding channel of the reaction $CH_3OO + HO_2$, but it has to be noted that for atmospheric conditions the HCHO-producing reaction channel should be negligible [*Lightfoot et al.*, 1992]. Another potential HCHO source to be discussed is downmixing of free tropospheric air. Unfortunately, measurements of vertical HCHO profiles in the remote marine troposphere are rare and hitherto published data indicate that the HCHO mixing ratios in the free troposphere tend to be lower than inside the MBL [*Arlander et al.*, 1995; *Zhou et al.*, 1996]. Since liquid-phase chemistry [*Lelieveld and Crutzen*, 1991] and HCHO deposition, which was not taken into account in our model, would make the situation even more unfavorable and variation of the H_2O_2 and HCHO deposition rates results in inconsistent H_2O_2 and HCHO mixing ratios, we suggest that the complex chemistry of the CH_3OO radical and MHP is not yet well understood. As mentioned in the introduction, a recent study by *Junkermann and Stockwell* [1999] indicates that methane photooxidation is sufficient to

Table 3. Comparison of the H_2O_2, MHP and HCHO Mixing Ratios Measured in the Subtropical NH (Average Values From 28°N-24°N) With Result of the Model Runs

	Measured Values (±σ)	Model Results:		
		Reaction Mechanism[a]	Modification[b]	Modification[c]
H_2O_2 [pptv]	1450±200	1250 (1360)	1320 (1680)	1280 (1450)
MHP [pptv]	590±220	1100 (1050)	610 (766)	710 (650)
HCHO [pptv]	580±160	330 (360)	410 (414)	380 (420)
MHP/HCHO (NO_x=12 pptv)	1.0±0.4	3.3	1.5	1.8
MHP/HCHO (NO_x=20 pptv)	-	2.9	1.8	1.5
MHP/(MHP+H_2O_2) NH	0.27	0.47	0.31	0.31
MHP/(MHP+H_2O_2) SH	0.34	0.48	0.36	0.37

The measured values correspond to daily means over this period. Simulations are made with the observed NO_x mixing ratio of 12 pptv and with 20 pptv (in parentheses). In addition, the calculated MHP/(MHP+H_2O_2) ratios for different CH_4/CO ratios typical for the NH and SH are shown (see text).

[a]Reaction mechanism shown in Tables 2a and 2b.

[b]Branching ratio of the reaction CH_3OO+HO_2 into the HCHO producing channel set to 0.4.

[c]Rate coefficients $k(CH_3OOH+OH)$ according to *Atkinson et al.* [1989] (see text).

describe the measured HCHO concentrations. However, their modeling required long-range transport of photochemically aged air masses from biomass burning regions in Africa. In contrast to our conditions, trajectories and weather charts indicate that such a special situation was given during their observation. As noted above, ethene and propene photochemistry may be an alternative explanation for the high HCHO levels measured during the *Albatross* campaign.

5. Conclusion

Hydroperoxide, formaldehyde, and NO/NO_2 measurements indicate that during the expedition the peroxy-radicals photochemistry was dominated by recombination and self reactions, while scavenging by NO was of minor importance. Only about 17% of the HCHO was typically formed via the reaction channel CH_3OO+NO. As a consequence, high MHP/HCHO ratios of about 0.9 were observed throughout the cruise. The dominant source of peroxy radicals was the photooxidation of CH_4 and CO, with probably negligible influence from NMHC photochemistry.

In regard to the hydroperoxide results, this campaign reveals that the results of the dual-enzyme and the HPLC method were generally in agreement on a ±25% level, although the sporatic discrepancies by a factor of 2 are somewhat disturbing. We attribute these inconsistencies to problems with the sampling efficiency and local effects due to different sampling positions on board. We emphasize that the reliability of the dual enzyme method in discriminating organic hydroperoxides and H_2O_2 is most probably only given if MHP is by far the dominant organic hydroperoxide. In regions where this premise is not given and organic hydroperoxides constitute a distinct part of the hydroperoxide budget, there is a need to employ alternative analytical techniques. Hydroperoxides are valuable indicators of free radical chemistry, but our investigations clearly demonstrate that apart from analytical problems conclusive results are complicated by the crucial and complex role of dry and wet deposition processes. In accord with previous studies we recommend an H_2O_2 deposition rate of around $(1.2\pm0.8)\times10^{-5}$ s^{-1} and tentatively a factor of 1.2-1.5 lower for MHP. However, the given uncertainties provoke a nearly comparable variance in the modeled steady state H_2O_2 and MHP mixing ratios, making budget considerations disturbingly uncertain. The need to study these processes more thoroughly has been already pointed out by *Martin et al.* [1997]. We suggest that deposition rates in the marine troposphere be determined preferentially at remote coastal observatories and not by shipborne measurements, where only special, hardly representative cases can be examined. Long-term observations, on the other hand, should provide more reliable deposition rates for different weather situations [*Ayers et al.*, 1996].

Concerning the HCHO distribution in the remote MBL, results from different field measurements provide an inconsistent picture. Our observed HCHO mixing ratios were higher by more than a factor of 3 than predicted by current photochemical theory, which is based on photooxidation of CO and CH_4. We are confident that this discrepancy can not be attributed to analytical problems. We have demonstrated that there is still a lack of understanding of the basic photochemical processes yielding HCHO in the very low NO_x regime. Model calculations point to the need of further kinetic and mechanistic studies of the methylperoxy radical and MHP chemistry, especially of the reaction $CH_3O_2+HO_2$. Apart from these problems the potential role of ethene and propene as being a significant HCHO source could not be considered appropriately. Although an obvious contribution of NMHC photochemistry on the hydroperoxide budget was not given, we cannot exclude a significant influence on the HCHO budget.

Acknowledgments. The authors thank the crew of RV *Polarstern* for their support aboard the ship and the Deutsche Wetterdienst (DWD) Offenbach for trajectory calculations We are very grateful to the meteorologists on board RV *Polarstern*, particularly L. Kaufeld, for assistance and helpful discussions. We thank the reviewers for valuable comments. This paper is contribution 1602 of the Alfred Wegener Institute for Polar and Marine Research.

References

Arlander, D.W., D Brüning, U. Schmidt, and D.H. Ehhalt, The tropospheric distribution of formaldehyde during TROPOZ II, *J. Atmos Chem*, *22*, 251-268, 1995.

Atkinson, R , D L. Baulch, R.A. Cox, R F Hampson Jr, J.A Kerr, and J. Troe, Evaluated kinetic and photochemical data for atmospheric chemistry· Supplement III, *J. Phys. Chem. Ref Data, 18*, 881, 1989.

Atkinson, R., D L. Baulch, R.A. Cox, R.F. Hampson Jr, J.A. Kerr, and J. Troe, Evaluated kinetic and photochemical data for atmospheric chemistry: Supplement IV. IFUAC subcommittee on gas kinetic data evaluation for atmospheric chemistry, *J. Phys. Chem. Ref. Data, 21*, 1125-1568, 1992

Ayers, G.P., S.A Penkett, R.W. Gillett, B Bandy, I.E. Galbally, C.P. Meyer, C M. Elsworth, S.T. Bentley, and B.W. Forgan, The annual cycle of peroxides and ozone in marine air at Cape Grim, Tasmania, *J. Atmos. Chem., 23*, 221-252, 1996.

Ayers, G.P , R.W. Gillett, C de Serves, and R.A. Cox, Formaldehyde production in clean marine air, *Geophys. Res Lett., 24*, 401-404, 1997

Barth, M.C., D A. Hegg, P.V. Hobbs, J.G. Walega, G.L. Kok, B.G. Heikes, and A.L. Lazrus, Measurements of atmospheric gas-phase and aqueous-phase hydrogen peroxide concentrations in winter on the east coast of the United States, *Tellus, Ser B, 41*, 61-69, 1989

Bonsang, B , C. Polle, and G. Lambert, Evidence for marine production of isoprene, *Geophys. Res. Lett., 19*, 1129-1132, 1992.

Burrows, J.P., P J. Crutzen, G.W. Harris, D. Klemp, T J Johnson, D. Perner, F.G. Wiehold, and T. Zenker, Messungen tropospharischer Spurengase mittels Dioden-Laser-Spektroskopie, BMFT Proj. 0744112, pp 1-34, Bundesminist für Forsch und Technol , Bonn, Germany, 1991.

Calvert, J G., and W R. Stockwell, Acid generation in the troposphere by gas phase chemistry, *Environ. Sci. Technol., 17*, 428A-443A, 1983.

Claiborn, C S., and V.P. Aneja, Measurements of atmospheric hydrogen peroxide in the gas phase and in cloud water at Mount Mitchell, North Carolina, *J Geophys. Res., 96*, 18,771-18,787, 1991.

Cohan, S.D , M.G Schultz, D J. Jacob, B.G. Heikes, and D.R. Blake, Convective injection and photochemical decay of peroxides in the tropical upper troposphere: Methyl iodide as a tracer of marine convection, *J. Geophys. Res., 104*, 5717-5724, 1999.

Cramer, G.L., J.F. Miller, R.B. Pendelton, and W.E.M. Lande, Iodometric measurements of lipid hydroperoxides in human plasma, *Anal. Biochem., 193*, 204-211, 1991.

Crutzen, P.J., and P.H. Zimmermann, The changing photochemistry of the troposphere, *Tellus, Ser. AB, 43*, 136-151, 1991.

Dasgupta, P K., S. Dong, H. Hwang, H.-C. Yang, and Z. Genfa, Continuous liquid-phase fluorometry coupled to a diffusion scrubber for real-time determination of atmospheric formaldehyde, hydrogen peroxide and sulfur dioxide, *Atmos. Environ., 22*, 949-963, 1988.

Deacon, E.L., Gas transfer to and across an air-water interface, *Tellus, 29*, 363-374, 1977.

DeMore, W.B., S.P. Sander, D.M. Golden, R.F. Hampson, M.J. Kurylo, C.J. Howard, A R. Ravishankara, C.E. Kolb, and M.J. Molina, Chemical kinetics and photochemical data for use in stratospheric modeling, Evaluation number 11, *JPL Publ., 94-26*, 1, 1994.

Gilge, S., D. Kley, and A. Volz-Thomas, Messungen von Wasserstoffperoxid und organischen Hydroperoxiden am Schauinsland im Schwarzwald - Ein Beitrag zur Charakterisierung der limitierenden Faktoren bei der Ozonproduktion, *Ber. Forsch. Julich 2998*, Forsch. Jülich, Julich, Germany, 1994.

Harris, G.W., D. Klemp, T. Zenker, and J.P. Burrows, Tunable diode laser measurements of trace gases during the 1988 *Polarstern* cruise and intercomparison with other methods, *J. Atmos. Chem.*, *15*, 315-326, 1992.

Heikes, B.G., Formaldehyde and hydroperoxides at Mauna Loa Observatory, *J. Geophys. Res.*, *97*, 18,001-18,013, 1992.

Heikes, B.G., G.L. Kok, J.G. Walega, and A.L. Lazrus, H_2O_2, O_3 and SO_2 measurements in the lower troposphere over the eastern United States during fall, *J. Geophys. Res.*, *92*, 915-931, 1987.

Heikes, B.G., M. Lee, D. Jacob, R. Talbot, J. Bradshaw, H. Singh, D. Blake, B. Anderson, H. Fuelberg, and A.M. Thompson, Ozone, hydroperoxides, oxides of nitrogen, and hydrocarbon budgets in the marine boundary layer over the South Atlantic, *J. Geophys. Res.*, *101*, 24,221-24,234, 1996.

Hellpointner, E., and S. Gäb, Detection of methyl, hydroxymethyl and hydroxyethyl hydroperoxides in air and precipitation, *Nature*, *337*, 631-634, 1989.

Jacob, P. and D. Klockow, Hydrogen peroxide concentration variations in the marine tropospheric atmosphere, in *Physico-Chemical Behavior of Atmospheric Pollutants*, edited by G. Restelli and G. Angeletti, pp. 638-643, Kluwer Acad., Norwell, Mass., 1990.

Jenkin, M.E., R.A. Cox, G.D. Hayman, and L.J. Whyte, Kinetic study of the reactions CH_3O_2+CH_3O_2 and CH_3O_2+HO_2 using molecular modulation spectroscopy, *J. Chem. Soc. Faraday Trans. 2*(84), 913-930, 1988.

Junkermann, W., and W.R. Stockwell, On the budget of photooxidants in the marine boundary layer of the tropical South Atlantic, *J. Geophys. Res.*, *104*, 8039-8046, 1999.

Kan, C.S., J.G. Calvert, and J.H. Shaw, Reactive channels of the CH_3O_2-CH_3O_2 reaction, *J. Phys. Chem.*, *84*, 3411-3417, 1980.

Kleindienst, T.E., et al., Comparison of techniques for measurement of ambient levels of hydrogen peroxide, *Environ. Sci. Technol.*, *22*, 53-61, 1988.

Kleinman, L.I., Low and high NO_x tropospheric photochemistry, *J. Geophys. Res.*, *99*, 16,831-16,838, 1994.

Kley, D., P.J. Crutzen, H.G.J. Smit, H. Vömel, S.J. Oltmans, H. Grassl, and V. Ramanathan, Observations of near-zero ozone concentrations over the convective Pacific: Effects on air chemistry, *Science*, *274*, 230-233, 1996.

Lazrus, A.L., G.L. Kok, S.N. Gittin, J.A. Lind, and S. McLaren, Automated fluorometric method for hydrogen peroxide in atmospheric precipitation, *Anal. Chem.*, *57*, 917-922, 1985.

Lee, M., B.G. Heikes, D.J. Jacob, G. Sachse, and B. Anderson, Hydrogen peroxide, organic hydroperoxide, and formaldehyde as primary pollutants from biomass burning, *J. Geophys. Res.*, *102*, 1301-1309, 1997.

Lelieveld, J., and P.J. Crutzen, The role of clouds in tropospheric photochemistry, *J. Atmos. Chem.*, *12*, 229-267, 1991

Lightfoot, P.D., R.A. Cox, J.N. Crowley, M. Destriau, G.D. Hayman, M.E. Jenkin, G.K. Moortgat, and F. Zabel, Organic peroxy radicals: Kinetics, spectroscopy and tropospheric chemistry, *Atmos. Environ., Part A*, *26*, 1805-1961, 1992.

Lind, J.A., and G.L. Kok, Henry's law determination for aqueous solutions of hydrogen peroxide, methylhydroperoxide, and peroxyacetic acid, *J. Geophys. Res.*, *91*, 7889-7895, 1986.

Lind, J.A., and G.L. Kok, Correction to Henry's law determination for aqueous solutions of hydrogen peroxide, methylhydroperoxide, and peroxyacetic acid, *J. Geophys. Res.*, *99*, 21,119, 1994.

Liss, P.S., and L. Merlivat, Air-sea gas exchange rates: Introduction and Synthesis in *The Role of Air-Sea Exchange in Geochemical Cycling*, edited by P. Buat-Ménard, pp 113-127, D. Reidel, Norwell, Mass., 1986.

Logan, J.A., M.J. Prather, S.C. Wofsy, and M.B. McElroy, Tropospheric chemistry: A global perspective, *J. Geophys. Res.*, *86*, 7210-7254, 1981.

Lowe, D.C., and U. Schmidt, Formaldehyde (HCHO) measurements in the nonurban atmosphere, *J. Geophys. Res.*, *88*, 10,844-10,858, 1983.

Martin, D., M. Tsivou, B. Bonsang, C. Abonnel, T. Carsey, M. Springer-Young, A. Pszenny, and K. Suhre, Hydrogen peroxide in the marine boundary layer during the Atlantic Stratocumulus Transition Experiment/Marine Aerosol and Gas Exchange experiment in the eastern North Atlantic, *J. Geophys. Res.*, *102*, 6003-6015, 1997.

McFarland, M., D. Kley, J.W. Drummond, A.L. Schmeltekopf, and R.H. Winkler, Nitric oxide measurements in the equatorial Pacific region, *Geophys. Res. Lett.*, *6*, 605-608, 1979.

Penkett, S.A., P.S. Monks, L.J. Carpenter, K.C. Clemitshaw, G.P. Ayers, R.W. Gillet, I.E. Galbally, and C.P. Meyer, Relationship between ozone photolysis rates and peroxy radical concentrations in clean marine air over the Southern Ocean, *J. Geophys. Res.*, *102*, 12,805-12,817, 1997.

Platt, U., J. Rudolph, T. Brauers, and G.W. Harris, Atmospheric measurements during Polarstern cruise ANT VII/1, 54°N to 32°S: An overview, *J. Atmos. Chem.*, *15*, 203-214, 1992.

Rohrer, F., and D. Brüning, Surface NO and NO_2 mixing ratios measured between 30°N and 30°S in the Atlantic region, *J. Atmos. Chem.*, *15*, 253-268, 1992.

Singh, H.B., and P.B. Zimmermann, Atmospheric distribution and sources of nonmethane hydrocarbons, in *Gaseous Pollutants: Characterization and Cycling*, edited by J.O. Nriagu, pp 177-235, John Wiley, New York, 1992.

Singh, H.B. et al., Low ozone in the marine boundary layer of the tropical Pacific Ocean: Photochemical loss, chlorine atoms, and entrainment, *J. Geophys. Res.*, *101*, 1907-1917, 1996.

Slemr, F., and H.G. Tremmel, Hydroperoxides in the marine troposphere over the Atlantic Ocean, *J. Atmos. Chem.*, *19*, 371-404, 1994.

Staffelbach, T., A. Neftel, B. Stauffer and D. Jacob, A record of the atmospheric methane sink from formaldehyde in polar ice cores, *Nature*, *349*, 603-605, 1991.

Staffelbach, T., A. Neftel, and P.K. Dasgupta, Artifact peroxides produced during cryogenic sampling of ambient air, *Geophys. Res. Lett.*, *22*, 2605-2608, 1995.

Staffelbach, T., G.L. Kok, B.G. Heikes, B. McCully, G.I. Mackay, D.R. Karecki, and H.I. Schiff, Comparison of hydroperoxide measurements made during the Mauna Loa Observatory Photochemistry Experiment 2, *J. Geophys. Res.*, *101*, 14,729-14,739, 1996.

Thompson, A.M., The oxidizing capacity of the Earth's atmosphere: Probable past and future changes, *Science*, *256*, 1157-1165, 1992.

Thompson, A.M., J.A. Chappellaz, I.Y. Fung, and T.L. Kucsera, The atmospheric CH_4 increase since the Last Glacial Maximum, 2, Interactions with oxidants, *Tellus, Ser. B*, *45*, 242-357, 1993a.

Thompson, A.M., et al., Ozone observations and a model of marine boundary layer photochemistry during SAGA 3, *J. Geophys. Res.*, *98*, 16,955-16,968, 1993b.

Torres, A.L., and A.M. Thompson, Nitric oxide in the equatorial pacific boundary layer: SAGA 3 Measurements, *J. Geophys. Res.*, *98*, 16,949-16,954, 1993.

Vaghjiani, G.L., and A.R. Ravishankara, Kinetics and mechanism of OH reaction with CH_3OOH, *J. Phys. Chem.*, *93*, 1948-1959, 1989.

Weller, R., and O. Schrems, H_2O_2 in the marine troposphere and seawater of the Atlantic Ocean (48°N-63°S), *Geophys. Res. Lett.*, *20*, 125-128, 1993.

Weller, R., and O. Schrems, Photooxidants in the marine Arctic troposphere in summer, *J. Geophys. Res.*, *101*, 9139-9147, 1996.

Weller, R., R. Lilischkis, O. Schrems, R. Neuber, and S. Wessel, Vertical ozone distribution in the marine atmosphere over the central Atlantic Ocean (56°S-50°N), *J. Geophys. Res.*, *101*, 1387-1399, 1996.

Williams, H. R. and H.S. Mosher, Organic peroxides, I, n-Alkyl hydroperoxides, *J. Am. Chem. Soc.*, *76*, 2984-2987, 1954.

Zafiriou, O.C., J. Alford, M. Herrera, E.T. Peltzer, R.G. Gagosian, and S.C. Liu, Formaldehyde in remote marine air: Flux measurements and estimates, *Geophys. Res. Lett.*, *7*, 341-344, 1980.

Zhou, X., Y.-N. Lee, L. Newman, X. Chen, and K. Mopper, Tropospheric formaldehyde concentration at the Mauna Loa Observatory during the Mauna Loa Observatory Photochemistry Experiment 2, *J. Geophys. Res.*, *101*, 14,711-14,719, 1996.

A. Boddenberg and S. Gäb, Fachbereich 9 - Analytische Chemie, Bergische Universität Gesamthochschule Wuppertal, 42097 Wuppertal, Germany. (e-mail: boddenbe@uni-wuppertal.de).

M. Gautrois, Institut für Atmosphärische Chemie ICG-3, Forschungszentrum Jülich GmbH, 52425 Jülich, Germany. (e-mail. m.gautrois@fz-juelich.de).

O. Schrems and R. Weller, Alfred Wegener Institut für Polar- und Meeresforschung, 27570 Bremerhaven, Germany. (e-mail: rweller@awi-bremerhaven.de).

(Received April 21, 1999; revised November 17, 1999;
accepted November 19, 1999.)